Fusion Engineering and Design 136 (2018) 1433–1437

Contents lists available at ScienceDirect

Fusion Engineering and Design

journal homepage: www.elsevier.com/locate/fusengdes

Investigation of vibrations caused by the steam condensation at sub-atmospheric condition in VVPSS

Rosa Lo Frano[a,*], Dahmane Mazed[a], Marco Olcese[b], Donato Aquaro[a], Daniele Del Serra[a], Igor Sekachev[b], Guglielmo Giambartolomei[a]

[a] University of Pisa, lg L. Lazzarino, Pisa, Italy
[b] ITER Organization, St Paul Lez Durance Cedex, France

ARTICLE INFO

Keywords:
ITER
VVPSS safety system
Vibration
Experiment
Steam condensation

ABSTRACT

Fusion technology deployment passes through the design of safety systems aimed to protect the Vacuum Vessel (VV) from pressurizing accidents event such as LOVA (Loss Of Vacuum Accident) or the failure of the Tokamak Water Cooling System (TWCS) causing the LOCA (Loss Of Coolant Accident). One of important safety systems of the ITER plant is the Vacuum Vessel Pressure Suppression System (VVPSS), which is designed to protect the VV by the steam condensation at sub-atmospheric pressure conditions in Suppression Tanks.

The aim of this study is to investigate vibrations phenomenon, originated during the steam-water direct contact condensation (DCC) at sub-atmospheric conditions, and determine any correlations between the steam jet dynamic and water temperature (T_W), steam mass flux (G_S) and downstream pressure (P_W).

According to the thermal hydraulic conditions characterising the DCC, vibrations may evolve because of the latent heat of the phase change (large amount of heat transmitted quickly to the water).

In the paper also presents the numerical investigations performed by means of proper FEM code, the set-up procedure and the experimental activity carried out at Lab. B. Guerrini of DICI- University of Pisa. This latter allowed correlating the different steam condensation regimes (chugging, condensation oscillation, etc.) to the acceleration and force, to be in turn used to determine the strength capacity of the VVPSS.

1. Introduction

The ITER Vacuum Vessel Pressure Suppression System (VVPSS) is a key safety component that limits the Vacuum Vessel (VV) internal pressure to 0.2 MPa, during in-vessel coolant leak events [1–3] and maintains the VV long-term pressure below atmospheric pressure during air or incondensable gases ingress.

The VVPSS configuration consists of 4 suppression tanks (ST), mounted together like indicated in Fig. 1, with an identical volume (100 m^3), inner diameter of 6.2 m and an overall height of about 4.7 m.

During an in-vessel coolant leak (Ingress of Coolant Event (ICE)) the VVPSS acts together with the VV drainage system, the former discharging evolved steam to the suppression tanks where it is condensed, while the latter facilitates drainage of water from the VV. As a consequence of that, it can be seen how steam direct contact condensation (DCC) of steam into the STs water is the thermal-hydraulic phenomenon that guarantees the VV pressure safety limit not to be exceeded in case of VV pressure build-up.

In fact, VVPSS operation conditions, characterized by slightly superheated steam condensed at very low, near vacuum, pressure and using water close to saturation conditions, are not standard for traditional fission nuclear power systems (operating at atmospheric pressure [4]); for this reason this topic is quite new in the nuclear field.

This study focuses on the vibrations, which were observed to evolve during the DCC experiments carried out, at sub-atmospheric pressure conditions, on a VVPSS prototype (scaled apparatus [3] of the real system).

Experimental tests are extremely important for the qualification of the VVPSS.

In Section 2 description of vibration oscillation is provided along with a brief description of the experimental apparatus properly set up to study the characteristics of the pressure oscillations.

In Section 3, the results of performed tests are presented. They provide the basis for the understanding of the phenomena occurring in the VVPSS for different sparger's configurations.

Oscillatory motion is thus correlated to the water temperature (T_W), steam mass flux (G_S) and downstream pressure (P_W).

* Corresponding author.
E-mail address: rosa.lofrano@ing.unipi.it (R. Lo Frano).

https://doi.org/10.1016/j.fusengdes.2018.05.031
Received 29 September 2017; Received in revised form 8 May 2018; Accepted 10 May 2018

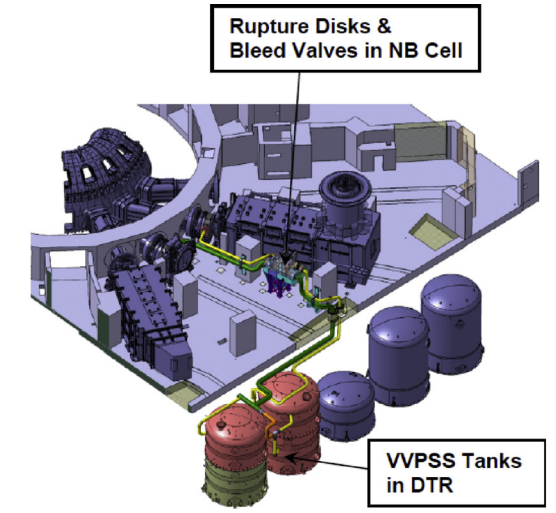

(a)

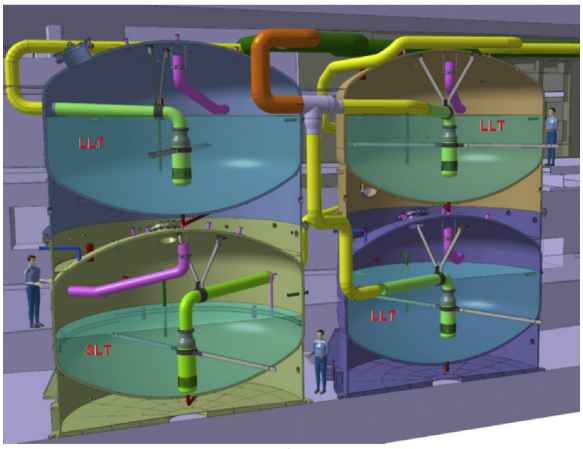

(b)

Fig. 1. a, b: (a) Part of plant layout view with DTR and VVPSS and (b) section view of STs with one Small Leak Tank – SLT (the tank at bottom left) and three Large Leak Tanks – LLTs (a tank at the top left, one at the bottom right and another at the top right) [5].

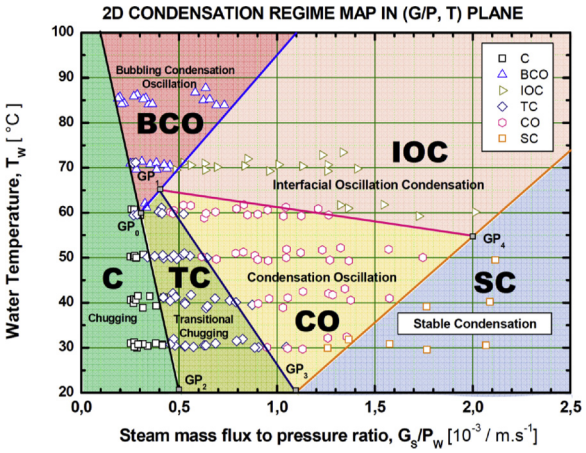

Fig. 2. Experimental 2D map with indication of the condensation regions, each one identified with a different color [5]. These regions are: Chugging (C); Transitional Chugging (TC); Condensation Oscillation (CO); Stable Condensation (SC); Bubbling Condensation Oscillation (BCO); Interfacial Oscillation Condensation (IOC).

2. Vibrations investigation

Vibrations are dynamic loads, which evolve during the DCC due to the "instant" heat transfer to the water.

It was observed during past experimental campaign that the vibrations are also characterised by: the Chugging (C) and the Condensation Oscillation (CO).

Fig. 2 shows the 2D map of condensation regimes experimentally determined (in [5] are provided further insights): it can be seen that unstable regimes appear at lower steam mass flux to downstream pressure ratio (G_S/P_W).

Stable Condensation (SC) is reached when a stationary jet plume develops and does not change neither in length nor in radial extension: SC regime is represented in Fig. 2 by the light blue domain, whose boundary is given by the equation:

$$T_{SC} = 38.9\frac{G}{P} - 22.8 \quad (1)$$

Fig. 3. CT elevation scheme with indication of the levels and types of measurement instrumentations.

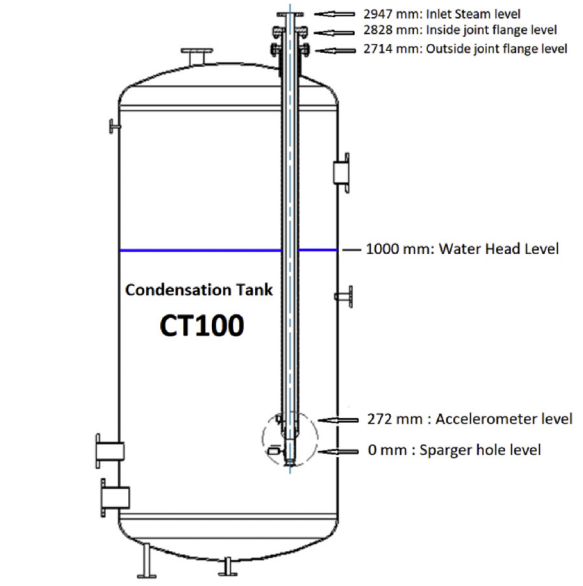

(a)

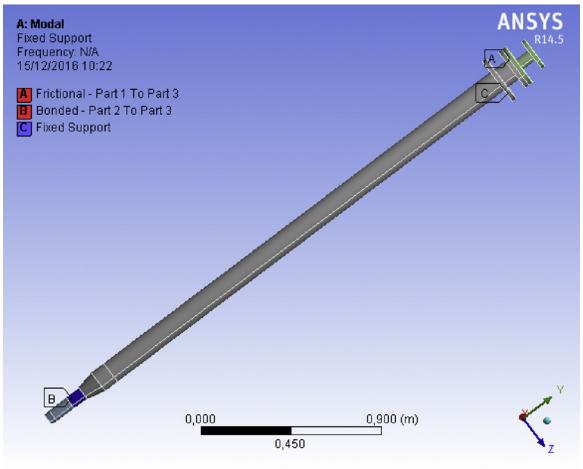

(b)

Fig. 4. Experimental CT sketch (a) and sparger FE model (b).

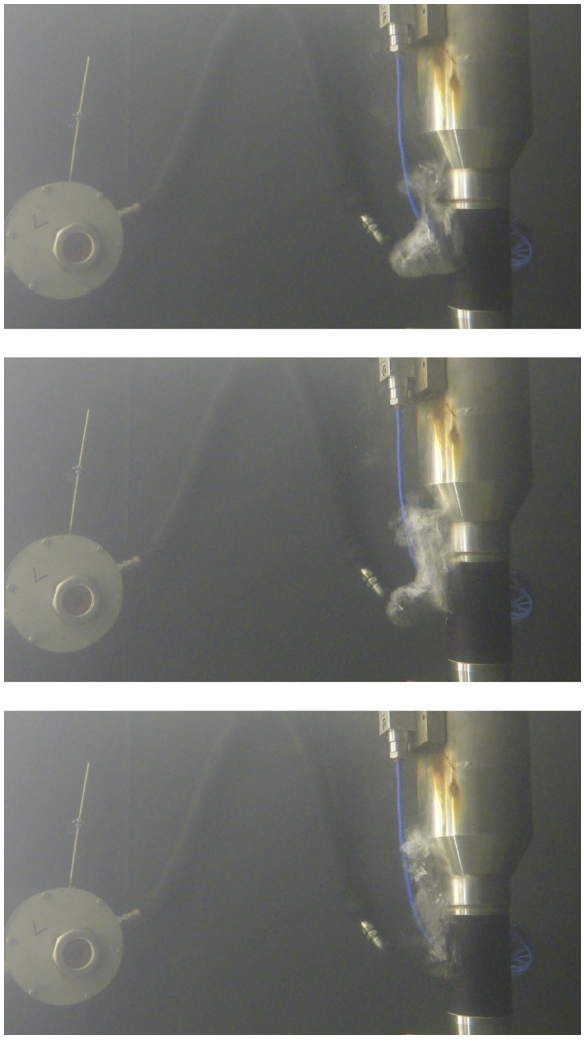

Fig. 5. Behavior of the steam condensation for exit hole patterns H_1 (T_w = 70 °C; 1 m water head level and average steam flow rate of 1.40 g/s). Duration of steam discharge was about 16 min.

SC appears then when the following condition is fulfilled:

$$\left\{ \begin{array}{c} \frac{G_S}{P_W} \geq 1.110^{-3} m^{-1} s \\ \text{and} \\ T_W \leq 38.9 \frac{G_S}{P_W} - 22.8 \end{array} \right\} \quad (2)$$

Unstable regimes may result in strong sparger loads triggered by pressure oscillations within the ST.

The large amplitude of the pressure oscillations may in turn generate high dynamic loads on the sparger system and impair the bearing capacity and the safe operation of the VVPSS.

Since dynamic loads (amplitude), that would have to arise in the suppression tank during DCC, are dependent on steam mass, temperature and frequency of oscillations, for a deep comprehension of the sparger vibrations (and pressure oscillations), more than 40 experimental tests have been performed.

For this aim, different sparger configuration (with single hole (H_1), two holes (H_2) and three holes (H_3)) are considered. Moreover, the H_1 sparger was appositely designed in order to provide a consistent reference case study.

As for the other two configurations (H_2 and H_3), the distance between the upper and the lower hole is set equal to 266 mm, just as actually envisaged in the full size sparger design of the ST.

2.1. Description of the test facility

Fig. 3 shows the Condensation Tank (CT), that is the main subsystem of the experimental facility [3,5] designed and built at the University of Pisa (volume scaling factor 1/21 respect the ITER ST) to allow the experimental tests on DCC phenomena and to monitor all the most affecting parameters.

To the purpose of the present study, the steam mass flux, the pressure and the temperature are considered not scaled down.

The CT is a stainless steel cylindrical vacuum tight vessel (with thermal insulation) deeply instrumented with 28 temperature sensors (± 0.1 °C) and 8 pressure transducers (± 0.1 kPa) accelerometer (with measuring range from 0 to 50 g) and strain gauges in order to monitor and measure the temperature and pressure throughout the water volume. The water head level is measured (± 1 mm) through a differential pressure sensor level.

The physical parameters characterizing the DCC are recorded by means of a Data Acquisition System (DAS), by LabVIEW©, and through a video recording system made of four high speed video cameras

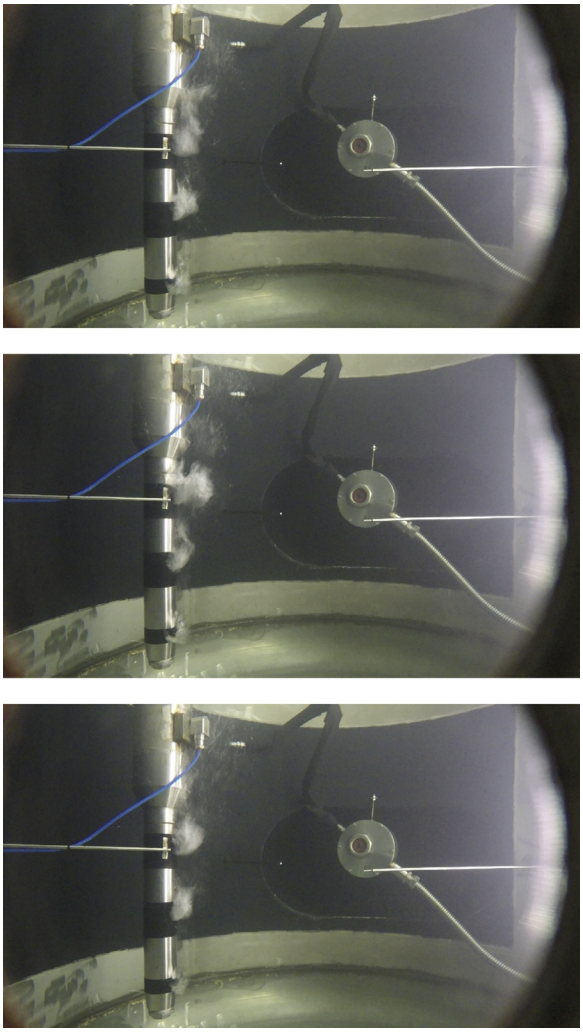

Fig. 6. Behavior of the steam condensation for exit hole patterns H_3 (T_w = 70 °C; 1 m water head level and average steam flow rate of 4.8 g/s). Duration of steam discharge was about 3 min.

(GOPRO Hero4 model type) installed inside the CT [3].

2.2. Experimental procedure

The mechanical vibrations induced on the sparger by the excitation force (F_{ext}) for a given condensation regime (Fig. 2) for a given exit hole pattern and thermal-hydraulic conditions, may be written as:

$$\ddot{x}(t) + 2\xi\omega_0\dot{x}(t) + \omega_0^2 x(t) = -F_{ext} \tag{3}$$

$$F_{ext} = \sum_{holes} \frac{q_s^2}{\rho_s A} f(\omega t) \tag{4}$$

In Eq. (3) ω_0 is the fundamental frequency of the sparger and ξ is the damping ratio. $\ddot{x}(t)$, $\dot{x}(t)$, and x(t) are the acceleration, the velocity and the displacement of the center of mass of the moving sparger.

In Eq. (4) A is the exit hole area, ρ_s is the density of steam at the exit hole and q_s is the steam flow rate.

The forcing frequency ω instead relates the stiffness and inertia of sparger to the condensation regime.

After that, we performed a modal analysis (by FEM code) on model shown in Fig. 4 in order to determine sparger first frequencies and vibration (bending) modes. The model of the sparger is made of SOLID187 element, 10-node element available in ANSYS code; each node has three degrees of freedom. Delaunay method allowed for mesh refinement. The labels A, B and C in Fig. 4b are representing the face-to-face contact and the real connection type of sparger to the CT. Modal analysis is solved with Lanczos algorithm.

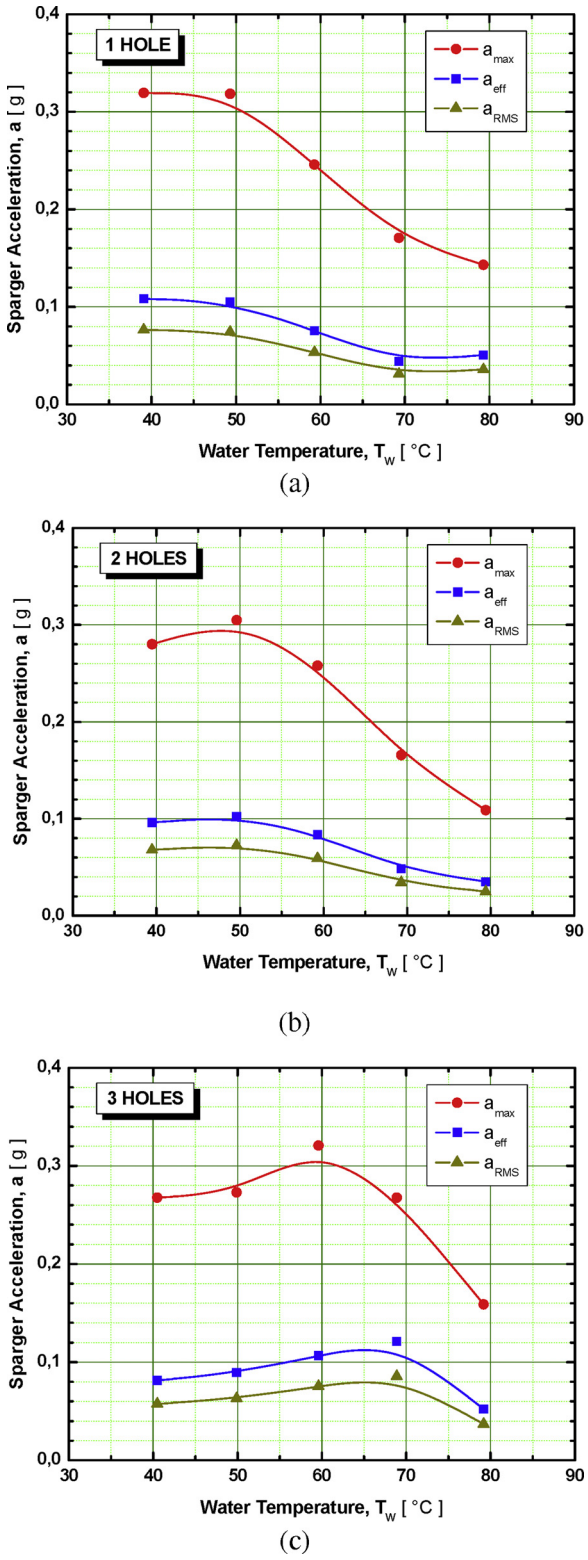

Fig. 7. Sparger acceleration versus water temperature for 1 hole (a), 2 holes (b) and (c) 3 holes pattern. Plots show the measured maximum acceleration (a_{max}), the effective sparger acceleration (a_{eff}), which is determined as mean maximum acceleration, and the acceleration root mean square (a_{RMS}), which represents the sparger vibration energy.

Based on the calculated frequencies we set-up a consistent

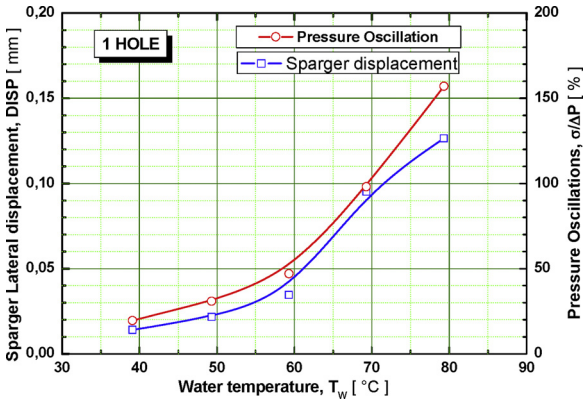

Fig. 8. Sparger lateral displacements and pressure oscillations as a function of water temperature.

experimental procedure to process measured signals. The Fast Fourier Transform (FFT) technique was used to convert time domain measured data into the frequency domain.

3. Experimental results

To characterize the sparger vibrations and the expected pressure oscillations during system operation, 40 experiments on DCC are performed by combining the following parameters:

- Initial water temperature (from 40 to 80 °C);
- Three exit hole patterns (H_1, H_2 and H_3);
- Five different steam condensation regimes (CR): C, BCO, CO, IOC, SC;
- Thirteen values of the main control variable, $X = G_S/P_w$, the steam mass flux to downstream pressure ratio.

The experimental data of sparger accelerations and the pressure oscillations have been analyzed through consistent Fast Fourier Transform (FFT) routines.

Oscillations (transverse oscillatory motion) during the steam condensation in water are due to the latent heat of the phase change. At the tail of the jet plume energy is lower because of the dissipation occurred during condensation at the interface and along the jet length.

Different steam condensation behaviours (Figs. 5 and 6) have been obtained for the same experimental test conditions that are 70 °C water pool temperature, 40 KPa downstream pressure, and similar mass flow rate per hole (G_S/P_W ratio are 0.43 ms/m and 0.51 ms/m).

The sparger design configuration hence affects the steam condensation behaviour as clearly confirmed by Figs. 5 and 6. The three sequential images of the steam jet at different time highlight the no-stable behavior of the BCO regime to which both tests belong (see Fig. 2).

Figs. 5 and 6 show thus the influence of the different sparger's configurations on the transverse oscillatory motion respectively in the Chugging and Condensation Oscillation.

The effective sparger acceleration is determined (by applying FFT) as function of the root mean square of acquired sparger acceleration data.

In particular, Fig. 7 shows the trends of the variation of the accelerations with the water temperature for H_1, H_2 and H_3 sparger pattern: the acceleration decreases as the pool water temperature increases.

All the curves exhibit the same dependence with respect to T_W, since the sparger acceleration (vibration energy) depends on the water subcooling and steam condensation regime.

Moreover the maximum sparger acceleration (~0.3 g at 50–60 °C) seemed to depend only on differential pressure $\Delta P = P_{Sparger}\text{-}P_{water}$.

The sparger displacement (Fig. 8) increases with T_w since it behaves like the inverse square of the mean vibration frequency.

At higher T_w the steam condensation regime moves towards Chugging/Bubbling flow patterns, even for low G_S/P_W resulting thus in pressure oscillation increase.

4. Conclusions

The performed experimental results of steam condensation at subatmospheric condition lead to the following conclusions:

- The amplitude of dynamic oscillations (pressure pulse) is dependent on the steam flow rate, water pool temperature and CR (through frequency of oscillations).
- The pressure oscillation decreases as G_S/P_W increases.
- The maximum sparger acceleration seems to depend only on $\Delta P = P_{Sparger}\text{-}P_{water}$. It decreases as the pool water temperature increases (with the same trend).
- Chugging/bubbling condensation oscillation may cause strong sparger loads triggered by pressure oscillations within the VVPSS Tank.

The pressure and force due to vibration will be added to determine the strength capacity of the VVPSS.

Disclaimer

The views and opinions expressed herein do not necessarily reflect those of the ITER Organization.

References

[1] R. Lo Frano, et al., Thermo-mechanical test rig for experimental evaluation of thermal conductivity of ceramic pebble beds, Fusion Eng. Des. 109–111 (2016) 383–388.
[2] R. Lo Frano, et al., Fluid dynamics analysis of loss of vacuum accident of ITER cryostat, Fusion Eng. Des. 109–111 (2016) 1302–1307.
[3] D. Mazed, et al., Experimental study of steam pressure suppression by condensation in a water tank at sub-atmospheric pressure, Proceedings ICONE24, June 26–30, Charlotte, North Carolina, 2016.
[4] S. Cho, et al., Characteristics of pressure oscillation induced by direct contact condensation of steam discharged through sparger in a pool of sub-cooled water, Proceedings of the Korean Nuclear Society Spring Meeting Pohang, Korea, 1999 (May).
[5] R. Lo Frano, et al., Experimental investigation of functional performance of a vacuum vessel pressure suppression system of ITER, Fusion Eng. Des. 122 (2017) 42–46.